ACS Energy LETTERS

Cite This: ACS Energy Lett. 2017, 2, 2591-2597

http://pubs.acs.org/journal/aelccp

LETTER

Polycation Binders: An Effective Approach toward Lithium Polysulfide Sequestration in Li–S Batteries

Haiping Su,[†,‡] Chengyin Fu,[‡] Yifan Zhao,[§] Donghui Long,[*,†] Licheng Ling,[†] Bryan M. Wong,[‡,§] Jun Lu,[*,∥] and Juchen Guo[*,‡,§]

[†]State Key Laboratory of Chemical Engineering, East China University of Science and Technology, Shanghai 200237, PR China
[‡]Department of Chemical and Environmental Engineering, University of California, Riverside, California 92521, United States
[§]Materials Science and Engineering Program, University of California, Riverside, California 92521, United States
[∥]Chemical Sciences and Engineering Division, Argonne National Laboratory, Argonne, Illinois 60439, United States

Supporting Information

ABSTRACT: Lithium polysulfide sequestration by polymeric binders in lithium–sulfur battery cathodes is investigated in this study. We prove polycations can effectively adsorb lithium polysulfides via Coulombic attraction between the positively charged backbone and the polysulfide anions. For the first time, we measure the simultaneous mass change of the sulfur cathodes with poly(diallyldimethylammonium triflate) (PDAT) and polyvinylpyrrolidone (PVP) binders during lithiation–delithiation using electrochemical quartz crystal microbalance (EQCM). The EQCM results demonstrate significantly higher mass gain with PDAT binder under identical conditions, providing direct evidence that PDAT is a superior binder. The advantage of polycation binders is also proved by charge–discharge cycling combined with ultraviolet–visible spectroscopy and X-ray photoelectron spectroscopy. With the PDAT binder and minimized electrolyte/sulfur weight ratio, we further demonstrate electrodes with high sulfur loading achieving 4.2 mAh cm^{-2} areal capacity.

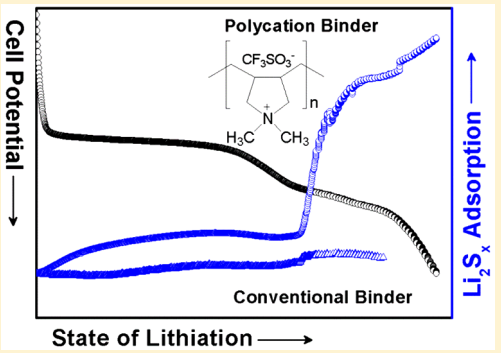

Rechargeable lithium–sulfur (Li–S) batteries are an attractive energy storage technology owing to the projected high specific energy.[1−3] To date, the commercialization of Li–S batteries is still hindered by key challenges arising from the intricate electrochemical processes that synergistically occur with both electrodes. Metallic Li anodes face critical safety concerns due to Li dendrite formation and are known to have inferior deposition–stripping efficiency and parasitic reactions in organic liquid electrolytes.[4−8] Consequently, significant excesses of Li and electrolytes are required in full cells at the expense of the cell specific energy.[9,10] On the other hand, sulfur cathodes suffer from fast capacity loss due to the dissolution of lithium polysulfides generated during the charge–discharge process. The dissolved polysulfides also induce polysulfide shuttle reactions,[11−14] which lead to low battery Coulombic efficiency (CE). Last but not the least, the amount of electrolyte used in full Li–S cells must be minimized to reduce the overall weight of the battery.[15−17]

Despite recent developments in innovative strategies such as sulfur subnano confinement[18−23] and utilizing solid-state electrolytes,[24−27] currently the most promising Li–S battery format from overall consideration of capacity, cost, and technical readiness is still the conventional cell composed of a metallic Li anode, a sulfur–carbon (S–C) composite cathode, and a liquid electrolyte. On the cathode side, although most of the research activities have been focused on the S–C composites, the polymer binder, which is an important component, recently has received increasing attention.[28−33] Effective binders should serve dual-functionality to promote polysulfide sequestration in addition to their conventional function for binding. In recent years, polyvinylpyrrolidone (PVP) has largely replaced polyvinylidene fluoride (PVDF) as the standard binder for sulfur cathodes.[28,34−37] It was proposed that heteroatoms such as oxygen and nitrogen could attract lithium polysulfides through the Coulombic interaction between the lone-pair electrons and Li^+ ions.[38−46] In addition to the heteroatom-containing polymers, ionomers including both polyanions and polycations have also been used as

Received: August 21, 2017
Accepted: October 6, 2017

DOI: 10.1021/acsenergylett.7b00779
ACS Energy Lett. 2017, 2, 2591−2597

binders.[28−30,47−53] To rationalize the selection of polymer binders, it is necessary to understand the electrochemical environment in the cathode−electrolyte interphase region. During discharge, the concentration profile of the soluble polysulfide anions (the active species) is under dynamic change: polysulfides have the highest concentration at the cathode−electrolyte interface (zero concentration in the bulk electrolyte at the beginning of the first discharge), which creates a strong concentration driving force for polysulfide diffusing into the bulk electrolyte. In addition to the concentration gradient, polysulfide anions are also repulsed from the negatively charged cathode surface during discharge. Therefore, an effective binder should be able to directly attract polysulfide anions via Coulombic attraction or other attractive interactions. We believe polycations, ionomers with a positively charged backbone, can be effective binders for sulfur cathodes.

To prove this hypothesis, we studied two representative polycation binders, namely poly[(2-ethyldimethylammonioethyl methacrylate ethyl sulfate)-*co*-(1-vinylpyrrolidone)] (polyquaternium D11) and poly(diallyldimethylammonium triflate) (PDAT) in comparison with the conventional PVP binder. Both D11 and PDAT are water-soluble ionomers containing quaternary ammonium cations on their backbones. D11 is commercially available, and its cation concentration is measured by elemental analysis (Table S1 in the Supporting Information). PDAT was obtained through an anion exchange reaction using poly(diallyldimethylammonium chloride) and silver triflate (CF_3SO_3Ag) as shown in Scheme 1. PVP, D11, and PDAT are all stable within the cycling window of Li−S batteries (Figure S1), and their properties are listed in Table 1. The key difference of these binders is their cation concentrations: PVP is uncharged; the cation concentration of D11 is 3.1×10^{-4} mol g^{-1}, and that of PDAT is more than 10 times higher at 3.6×10^{-3} mol g^{-1}. It is also worth noting that D11 is a copolymer containing a majority of PVP segments.

Scheme 1. Molecular Structures of Polyvinylpyrrolidone (PVP) and Poly[(2-ethyldimethylammonioethyl methacrylate ethyl sulfate)-co-(1-vinylpyrrolidone)] (D11) and the Synthesis of Poly(diallyldimethylammonium triflate) (PDAT) via Anion Exchange

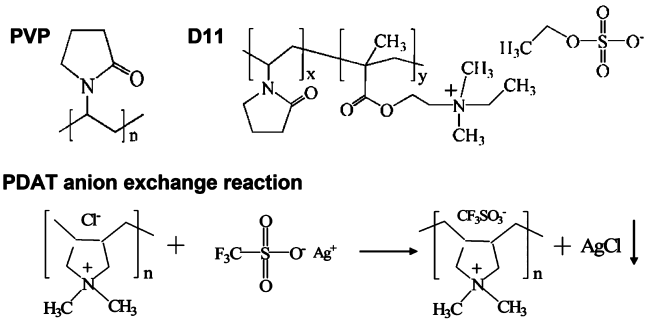

Table 1. Properties of Three Binders in This Study

binder	molecular weight (g mol^{-1})	cation concentration (mol g^{-1})
PVP	1 300 000	0
D11 (*x*:*y* = 26:1)	1 000 000	3.1×10^{-4}
PDAT	500 000	3.6×10^{-3}

The three binders was evaluated in S−C composite cathodes with ethereal electrolyte composed of 1 M lithium bis(trifluoromethylsulfonyl)imide (LiTFSI) in a mixture of 1,2-dioxolane (DOL) and dimethoxymethane (DME) (1:1 by volume) with 1.5 wt % $LiNO_3$. The porous carbon host material was synthesized with a sol−gel method using graphene oxide template (denoted as GO@C) as detailed in the Supporting Information. The S-GO@C composite contained 74 wt % of sulfur, and the electrodes were composed of 80 wt % composite, 10 wt % carbon black, and 10 wt % binder, namely PVP, D11, or PDAT. An electrolyte/sulfur (E/S) weight ratio of 60/1 (50 μL of electrolyte to 1 mg of sulfur) was used in the cycling. Such a high E/S ratio was intentionally employed to promote lithium polysulfide dissolution, providing a rigorous test of polysulfide sequestration by these binders. A relatively low discharge−charge current density of 160 mA g^{-1} (0.1 C) was also used for the same purpose. To demonstrate an unambiguous comparison, the cycling data for each binder were the average of five individual cathodes tested under the same conditions. As shown in Figure 1, both D11 and PDAT binders

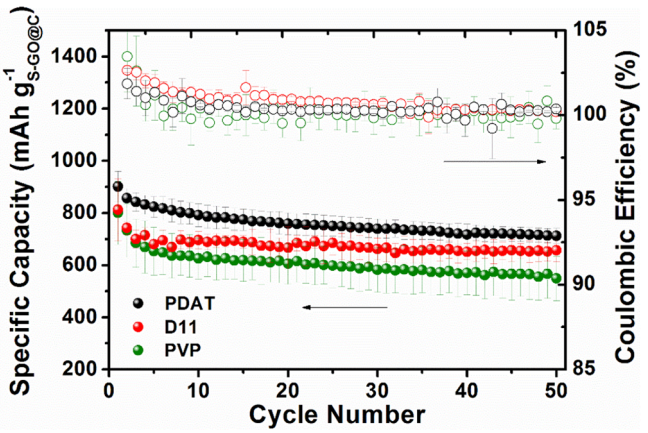

Figure 1. Cycle performance and Coulombic efficiency of S-GO@C cathodes with PVP, D11, and PDAT binders and E/S ratio of 60 under 0.1 C.

demonstrate a clear advantage over PVP in terms of overall capacity and cycle stability. S-GO@C cathodes with a D11 binder have initial discharge capacity similar to that of those with a PVP binder around 800 mAh g^{-1} (1081 mAh g^{-1} based on sulfur) but superior cycle stability. As mentioned above, D11 contains a majority of PVP segments; thus, the improvement of stability can obviously be attributed to the cationic segments. Notably, S-GO@C cathodes with PDAT binder exhibit an initial capacity at 900 mAh g^{-1} (1216 mAh g^{-1} based on sulfur), which is higher than that of PVP and D11. The cycle stability of S-GO@C with PDAT binder is also improved in the first few cycles. It is unambiguous that the polycation binders indeed demonstrate improved cycling performance compared the uncharged PVP binder.

The capability of PDAT to effectively adsorb polysulfide anions was further demonstrated from a direct comparison with PVP in adsorption experiments. Binder-GO@C composites (PVP-GO@C and PDAT-GO@C) were first prepared with a weight ratio of 1:2, which is the same ratio in the S-GO@C cathodes. The 20 mg of the respective binder-GO@C composites were added into 5 mL of 2 mM Li_2S_8 solution, immediately followed by filtration to remove the adsorbents. The contact time between the adsorbents and the Li_2S_8

DOI: 10.1021/acsenergylett.7b00779
ACS Energy Lett. 2017, 2, 2591−2597

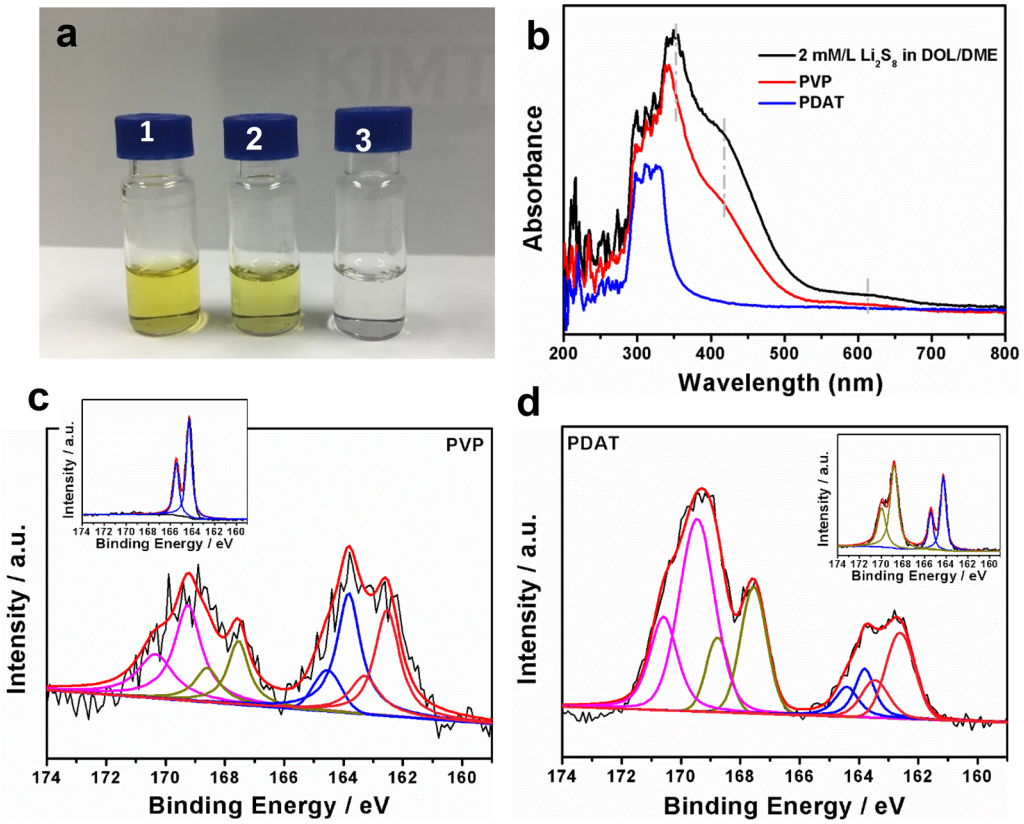

Figure 2. (a) Photographs of (1) 2 mM Li_2S_8 in DOL/DME (1:1 by volume) and the same solutions filtered with (2) PVP and (3) PDAT adsorbents; (b) UV−vis spectra of the 2 mM Li_2S_8 solution in DOL/DME before and after polysulfide removal by PVP and PDAT adsorbents; S 2p XPS spectra of lithiated S-GO@C electrodes with (c) PVP binder and (d) PDAT binder. The insets are the respective pristine S-GO@C electrodes.

solution was kept under 1 min to emphasize the effectiveness. The photographs of the pristine Li_2S_8 solution and the two Li_2S_8 solutions after adsorbing are shown in Figure 2a. The filtered Li_2S_8 solution using PVP-GO@C adsorbent changed to a slightly lighter yellow color. In stark contrast, the filtered Li_2S_8 solution using PDAT-GO@C adsorbent became completely colorless. The filtered solutions were subsequently investigated using ultraviolet−visible (UV−vis) spectroscopy with the pristine Li_2S_8 solution as the reference. As shown in Figure 2b, the main difference in their UV−vis spectra is in the peaks at 350, 430, and 610 nm, which represent the existence of S_6^{2-}, S_5^{2-}/S_6^{2-} anions, and $S_3^{\bullet-}$ free radical,[54,55] respectively. The pristine Li_2S_8 solution shows the strongest absorbance, whereas the Li_2S_8 solution with PVP-GO@C adsorbent shows a slightly reduced absorbance. In contrast, no absorbance at the wavelength of interest can be observed in the Li_2S_8 solution with PDAT-GO@C adsorbent, indicating a much stronger attraction between polysulfides and the polycation PDAT binder.

The advantage of PDAT over PVP binder was further verified by analysis of the composition of the lithiated S-GO@C cathodes with X-ray photoelectron spectroscopy (XPS) S 2p spectra shown in Figure 2c,d. The pristine S-GO@C electrode with PVP binder (inset in Figure 2c) shows a pure sulfur twin-peak at 164.0 eV (S $2p_{3/2}$) and 165.2 eV (S $2p_{1/2}$), while the additional twin-peak at 170.0 and 168.8 eV from the pristine electrode with PDAT binder (inset in Figure 2d) can be attributed to the triflate anion in PDAT.[56−58] After lithiation, both electrodes show a new twin-peak at 162.0 and 163.2 eV, which can be assigned as lithium sulfide (Li_2S).[59] No other polysulfide species were observed because of the spontaneous disproportionation to sulfur and Li_2S upon drying.[60,61] The percentages of pure sulfur and Li_2S in the lithiated samples with PDAT and PVP are distinctly different, as indicated by the integrated peak area. Only 37.7% of the sulfur in lithiated S-GO@C with PDAT binder remains as elemental sulfur, and the content of sulfur as Li_2S is 62.3%. In contrast, 51.4% of the sulfur in lithiated S-GO@C with PVP binder still remains as elemental sulfur, and the content of sulfur as Li_2S is 48.6%. The much higher Li_2S content in the cathode with the PDAT binder clearly indicates superior sulfur utilization, which is consistent with the stronger polysulfide adsorption of the PDAT binder.

To further confirm the effectiveness of polycation binders to sequestrate polysulfides, we performed electrochemical quartz crystal microbalance (EQCM) experiments on the S-GO@C cathodes with PVP and PDAT binders. The EQCM technique can simultaneously measure the mass changes on the oscillating quartz crystal electrode during electrochemical processes by monitoring the resonant frequencies.[62,63] The change of frequency of the quartz crystal electrode is correlated to the mass change by the Sauerbrey equation (Experimental Section in the Supporting Information). In our experiments, the mass change of the S-GO@C electrodes with the two binders (PVP vs PDAT) were measured during two electrochemical analyses: cyclic voltammetry (CV) and constant-current lithiation. Both experiments were performed in a three-electrode cylindrical cell with Li reference electrode, Li counter electrode, and the gold-coated quartz crystal working electrode, which was coated with

DOI: 10.1021/acsenergylett.7b00779
ACS Energy Lett. 2017, 2, 2591−2597

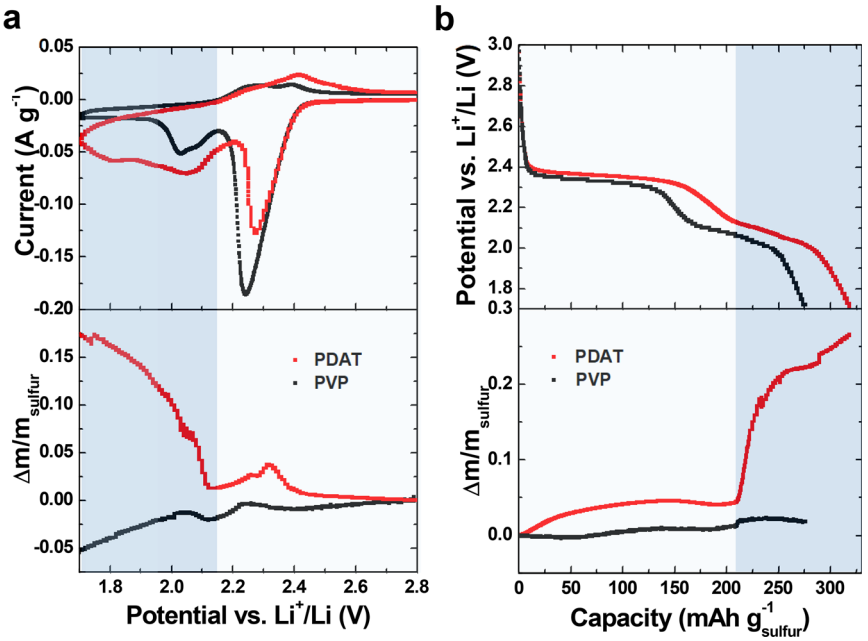

Figure 3. (a) CV (0.5 mV s^{-1}) and (b) constant-current lithiation (800 mA g^{-1}) curves and the corresponding mass changes measured by EQCM during the lithiation process of S-GO@C with PDAT and PVP binders.

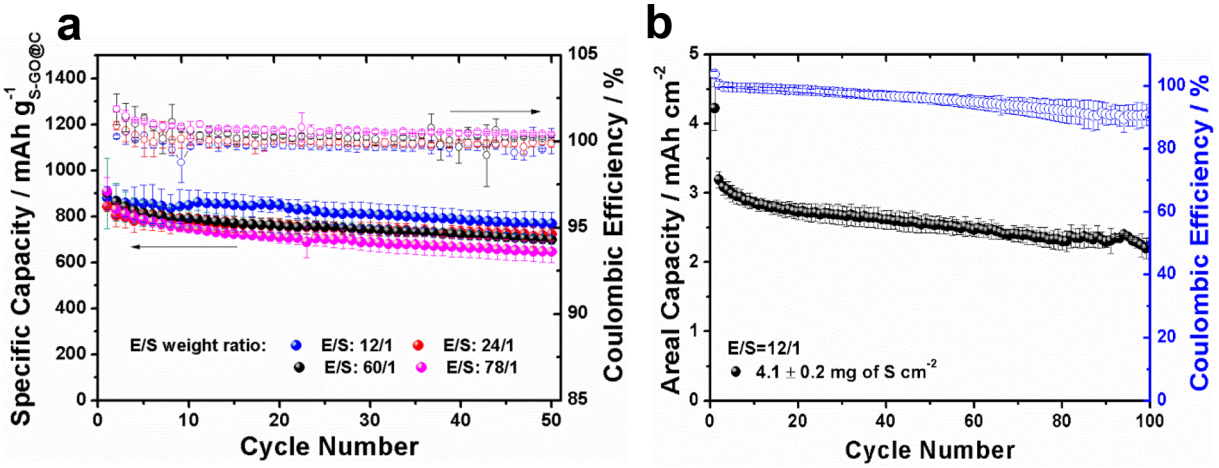

Figure 4. (a) Effects of the E/S weight ratio on cycling performance and Coulombic efficiency of S-GO@C cathode with PDAT binder under 0.1 C; (b) areal capacity, cycle stability, and Coulombic efficiency of S-GO@C thick electrodes with PDAT binder and E/S ratio of 12.

the S-GO@C with PVP or PDAT binder. It is necessary to mention that the electrolyte was in significant excess (with an E/S weight ratio around 4000/1) because of the structure of the cell. The CV curves of the S-GO@C electrodes with PVP and PDAT binders are shown at the top of Figure 3a, and the simultaneous mass changes during the cathodic scan are shown at the bottom. Due to the high E/S ratio in the three-electrode cell, the second cathodic peak (further lithiation of soluble polysulfides generated in the first cathodic peak) and the anodic peaks are diminished. Nevertheless, the simultaneous mass change curve of the electrode with the PDAT binder clearly displays a mass gain at the first cathodic peak around 2.3 V, which represents the formation of high-order soluble polysulfides. Following a slight mass loss between 2.3 and 2.1 V, the mass of the electrode continuously increased due to the formation of lower-order polysulfides and/or solid products Li_2S/Li_2S_2. On the other hand, the electrode with PVP binder shows continuous mass loss during the entire lithiation scan, which clearly represents more polysulfides dissolved into the electrolyte compared to the one with PDAT binder. In addition to CV scans, the constant-current lithiation curves and the simultaneous mass change curves of these two electrodes demonstrated the same behavior as shown in Figure 3b. Despite the low capacity achieved by the lithiation (again, due to the large amount of electrolyte), the significantly greater mass gain with the PDAT binder confirmed that polycation binders undoubtedly promotes polysulfide sequestration, thus improving cycle stability.

In addition to the polycation binders with polysulfide sequestration functionality, one less-investigated but very important parameter in Li−S batteries is the E/S ratio. The electrolyte is an indispensable component in a battery, but its weight percentage in the full cell must be minimized. The polycation binder characterizations so far in this study utilize a high E/S ratio of at least 60/1 to rigorously test the polysulfide sequestration; however, it is too high to be practical in Li−S

DOI: 10.1021/acsenergylett.7b00779
ACS Energy Lett. 2017, 2, 2591−2597

cells. Our calculation based on the full cell configuration suggested the E/S ratio must be lower than 3/1 to deliver a Li−S battery with a specific energy reaching 500 Wh kg^{-1}.[64] Therefore, we hereby demonstrate the effect of the E/S ratio on the S-GO@C cathode with the PDAT binder. As shown by the average cycle stability data (from 5 individual cathodes) in Figure 4a, Li−S coin cells with a higher E/S ratio of 78/1 clearly show cycle stability inferior to that of the cells with an E/S ratio of 60/1. The E/S ratio of 78/1 also demonstrated the worst CE, which is higher than 100%, although the potential causes for the >100% CE are not currently clear. When the E/S ratio is lowered from 60/1 to 24/1, the cycle stability as well as the CE was improved. We further lowered the E/S ratio to 12/1, which shows the best cycle stability. However, the CE from an E/S ratio of 12/1 becomes <100%. As such, the CE decreases with a concomitant decrease in the E/S ratio; however, a straightforward reasoning for this observation is not currently apparent. When we attempted to further lower the E/S ratio, unfortunately the cathode performance drastically decreased. We tentatively have three hypotheses about the failed attempt to further lower the E/S ratio: (1) Sufficient electrolyte is required to dissolve polysulfide species to achieve fast kinetics, i.e., when the E/S ratio is too low to effectively dissolve polysulfides, the voltage polarization becomes significant. (2) The nanostructure nature of the S-GO@C composite inherently requires a high amount of electrolyte for electrode wetting. This aspect also correlates with the electrode surface wettability to the electrolyte. (3) A coin cell may not be the optimal form for minimizing the E/S ratio because of the inevitable open space in the cell. Therefore, we will proceed with a pouch cell form to investigate strategies for further lowering the E/S ratio to an acceptable level for high-capacity Li−S batteries. Nevertheless, our results on the E/S ratio clearly indicate that a lower E/S ratio is not only critical for reducing the total weight of the battery but also closely correlated to the cycle stability and CE.

With the effective PDAT binder and the low E/S ratio of 12/1, we demonstrate the thick S-GO@C cathodes with practical sulfur loading at ∼4 mg cm^{-2}. Figure 4b shows the electrochemical performance (from triplicate) of S-GO@C with an average sulfur loading of 4.1 mg cm^{-2}. The first cycle was performed under 0.02 C (32 mA g^{-1}) delivering a capacity of 4.2 mAh cm^{-2}. The cathodes were subsequently cycled at 0.1 C from the second cycle delivering a capacity of 3.2 mAh cm^{-2}. The cathodes with high sulfur loading can retain a capacity of 2.1 mAh cm^{-2} after 100 discharge−charge cycles due to the effective sequestration of lithium polysulfides.

In summary, we unambiguously demonstrate that polycations are superior binder materials for lithium polysulfide sequestration via combined electrochemical and spectroscopic analyses. The low weight ratio of electrolyte to sulfur is a key parameter for ensuring a high specific energy of the full Li−S cells. We demonstrate that a lower E/S ratio is also beneficial for improving cathode cycle stability. Our study provides the necessary first step toward a rational guidance for sulfur cathode design; however, additional work to fine-tune the material properties is necessary. Specifically, the effects of the polycation binder properties including ion concentration and chemistry, molecular structure, and molecular weight need to be systematically investigated. In addition, the morphology, size, and surface polarity/wettability of the sulfur−carbon composites need to be optimized to further increase the sulfur loading and lower the E/S ratio. The development of a Li−S full cell must synergistically consider all three major components, including the sulfur cathode, electrolyte, and Li anode, of which the latter two will be the emphases of our future work.

■ ASSOCIATED CONTENT

Supporting Information

The Supporting Information is available free of charge on the ACS Publications website at DOI: 10.1021/acsenergylett.7b00779.

Experimental section, sulfur content analysis in polyquaternium, N_2 adsorption−desorption isotherms of the GO@C carbon hosts, SEM images and structural properties of GO@C carbon hosts, TGA of S-GO@C composites, cycle stability and Coulombic efficiency comparison of S-GO@C composites, SEM image of high-loading S-GO@C electrode on porous carbon paper, and capacity of high-loading S-GO@C electrode on Al current collector (PDF)

■ AUTHOR INFORMATION

Corresponding Authors

*E-mail: junlu@anl.gov.
*E-mail: longdh@mail.ecust.edu.cn.
*E-mail: jguo@engr.ucr.edu.

ORCID

Bryan M. Wong: 0000-0002-3477-8043
Jun Lu: 0000-0003-0858-8577
Juchen Guo: 0000-0001-9829-1202

Notes

The authors declare no competing financial interest.

■ ACKNOWLEDGMENTS

H.S. is grateful to the Chinese Scholarship Council for the visiting fellowship. This research has been supported by the Assistant Secretary for Energy Efficiency and Renewable Energy, Office of Vehicle Technologies of the U.S. Department of Energy through the Advanced Battery Materials Research (BMR) Program (Battery500 Consortium). The XPS was performed at the UC Irvine Materials Research Institute (IMRI) using instrumentation funded in part by the National Science Foundation Major Research Instrumentation Program under Grant No. CHE-1338173.

■ REFERENCES

(1) Evers, S.; Nazar, L. F. New approaches for high energy density lithium-sulfur battery cathodes. *Acc. Chem. Res.* **2013**, *46*, 1135−1143.
(2) Seh, Z. W.; Sun, Y.; Zhang, Q.; Cui, Y. Designing high-energy lithium-sulfur batteries. *Chem. Soc. Rev.* **2016**, *45*, 5605−5634.
(3) Manthiram, A.; Fu, Y.; Chung, S. H.; Zu, C.; Su, Y. S. Rechargeable lithium-sulfur batteries. *Chem. Rev.* **2014**, *114*, 11751−11787.
(4) Gireaud, L.; Grugeon, S.; Laruelle, S.; Yrieix, B.; Tarascon, J. M. Lithium metal stripping/plating mechanisms studies: A metallurgical approach. *Electrochem. Commun.* **2006**, *8*, 1639−1649.
(5) Kim, H.; Jeong, G.; Kim, Y. U.; Kim, J. H.; Park, C. M.; Sohn, H. J. Metallic anodes for next generation secondary batteries. *Chem. Soc. Rev.* **2013**, *42*, 9011−34.
(6) Xu, W.; Wang, J.; Ding, F.; Chen, X.; Nasybulin, E.; Zhang, Y.; Zhang, J. G. Lithium metal anodes for rechargeable batteries. *Energy Environ. Sci.* **2014**, *7*, 513−537.

DOI: 10.1021/acsenergylett.7b00779
ACS Energy Lett. 2017, 2, 2591−2597

(7) Qian, J.; Henderson, W. A.; Xu, W.; Bhattacharya, P.; Engelhard, M.; Borodin, O.; Zhang, J. G. High rate and stable cycling of lithium metal anode. *Nat. Commun.* **2015**, *6*, 6362.
(8) Li, W.; Yao, H.; Yan, K.; Zheng, G.; Liang, Z.; Chiang, Y. M.; Cui, Y. The synergetic effect of lithium polysulfide and lithium nitrate to prevent lithium dendrite growth. *Nat. Commun.* **2015**, *6*, 7436.
(9) Yang, Y.; McDowell, M. T.; Jackson, A.; Cha, J. J.; Hong, S. S.; Cui, Y. New nanostructured Li_2S/silicon rechargeable battery with high specific energy. *Nano Lett.* **2010**, *10*, 1486−1491.
(10) Hagen, M.; Hanselmann, D.; Ahlbrecht, K.; Maça, R.; Gerber, D.; Tübke, J. Lithium-sulfur cells: the gap between the state-of-the-art and the requirements for high energy battery cells. *Adv. Energy Mater.* **2015**, *5*, 1401986.
(11) Yin, Y. X.; Xin, S.; Guo, Y. G.; Wan, L. J. Lithium-sulfur batteries: electrochemistry, materials, and prospects. *Angew. Chem., Int. Ed.* **2013**, *52*, 13186−13200.
(12) Pang, Q.; Liang, X.; Kwok, C. Y.; Kulisch, J.; Nazar, L. F. A comprehensive approach toward stable lithium−sulfur batteries with high volumetric energy density. *Adv. Energy Mater.* **2017**, *7*, 1601630.
(13) Lv, D.; Zheng, J.; Li, Q.; Xie, X.; Ferrara, S.; Nie, Z.; Mehdi, L. B.; Browning, N. D.; Zhang, J. G.; Graff, G. L.; et al. High energy density lithium-sulfur batteries: challenges of thick sulfur cathodes. *Adv. Energy Mater.* **2015**, *5*, 1402290.
(14) Qie, L.; Manthiram, A. High-energy-density lithium−sulfur batteries based on blade-cast pure sulfur electrodes. *ACS Energy Lett.* **2016**, *1*, 46−51.
(15) Zhang, S. Improved cyclability of liquid electrolyte lithium/sulfur batteries by optimizing electrolyte/sulfur ratio. *Energies* **2012**, *5*, 5190−5197.
(16) Zheng, J.; Lv, D.; Gu, M.; Wang, C.; Zhang, J. G.; Liu, J.; Xiao, J. How to obtain reproducible results for lithium sulfur batteries? *J. Electrochem. Soc.* **2013**, *160*, A2288−A2292.
(17) Fang, R.; Zhao, S.; Hou, P.; Cheng, M.; Wang, S.; Cheng, H. M.; Liu, C.; Li, F. 3D interconnected electrode materials with ultrahigh areal sulfur loading for Li-S batteries. *Adv. Mater.* **2016**, *28*, 3374−3382.
(18) Je, S. H.; Hwang, T. H.; Talapaneni, S. N.; Buyukcakir, O.; Kim, H. J.; Yu, J. S.; Woo, S. G.; Jang, M. C.; Son, B. K.; Coskun, A.; et al. Rational sulfur cathode design for lithium−sulfur batteries: sulfur-embedded benzoxazine polymers. *ACS Energy Lett.* **2016**, *1*, 566−572.
(19) Xin, S.; Gu, L.; Zhao, N. H.; Yin, Y. X.; Zhou, L. J.; Guo, Y. G.; Wan, L. J. Smaller sulfur molecules promise better lithium-sulfur batteries. *J. Am. Chem. Soc.* **2012**, *134*, 18510−18513.
(20) Wu, H. B.; Wei, S.; Zhang, L.; Xu, R.; Hng, H. H.; Lou, X. W. Embedding sulfur in MOF-derived microporous carbon polyhedrons for lithium-sulfur batteries. *Chem. - Eur. J.* **2013**, *19*, 10804−10808.
(21) Zhang, B.; Qin, X.; Li, G. R.; Gao, X. P. Enhancement of long stability of sulfur cathode by encapsulating sulfur into micropores of carbon spheres. *Energy Environ. Sci.* **2010**, *3*, 1531−1537.
(22) Fu, C.; Wong, B. M.; Bozhilov, K. N.; Guo, J. Solid state lithiation−delithiation of sulphur in sub-nano confinement: a new concept for designing lithium−sulphur batteries. *Chem. Sci.* **2016**, *7*, 1224−1232.
(23) Li, Z.; Jiang, Y.; Yuan, L.; Yi, Z.; Wu, C.; Liu, Y.; Strasser, P.; Huang, Y. A highly ordered meso@ microporous carbon-supported sulfur@ smaller sulfur core−shell structured cathode for Li−S batteries. *ACS Nano* **2014**, *8*, 9295−9303.
(24) Lee, J. T.; Eom, K.; Wu, F.; Kim, H.; Lee, D. C.; Zdyrko, B.; Yushin, G. Enhancing the stability of sulfur cathodes in Li−S cells via in situ formation of a solid electrolyte layer. *ACS Energy Lett.* **2016**, *1*, 373−379.
(25) Marmorstein, D.; Yu, T.; Striebel, K.; McLarnon, F.; Hou, J.; Cairns, E. Electrochemical performance of lithium/sulfur cells with three different polymer electrolytes. *J. Power Sources* **2000**, *89*, 219−226.
(26) Hassoun, J.; Scrosati, B. Moving to a solid-state configuration: a valid approach to making lithium-sulfur batteries viable for practical applications. *Adv. Mater.* **2010**, *22*, 5198−5201.
(27) Lin, Z.; Liang, C. Lithium−sulfur batteries: from liquid to solid cells. *J. Mater. Chem. A* **2015**, *3*, 936−958.
(28) Seh, Z. W.; Zhang, Q.; Li, W.; Zheng, G.; Yao, H.; Cui, Y. Stable cycling of lithium sulfide cathodes through strong affinity with a bifunctional binder. *Chem. Sci.* **2013**, *4*, 3673.
(29) Li, G.; Ling, M.; Ye, Y.; Li, Z.; Guo, J.; Yao, Y.; Zhu, J.; Lin, Z.; Zhang, S. Acacia senegal-inspired bifunctional binder for longevity of lithium-sulfur batteries. *Adv. Energy Mater.* **2015**, *5*, 1500878.
(30) Wang, J.; Yao, Z.; Monroe, C. W.; Yang, J.; Nuli, Y. Carbonyl-β-Cyclodextrin as a novel binder for sulfur composite cathodes in rechargeable lithium batteries. *Adv. Funct. Mater.* **2013**, *23*, 1194−1201.
(31) Ai, G.; Dai, Y.; Ye, Y.; Mao, W.; Wang, Z.; Zhao, H.; Chen, Y.; Zhu, J.; Fu, Y.; Battaglia, V.; et al. Investigation of surface effects through the application of the functional binders in lithium sulfur batteries. *Nano Energy* **2015**, *16*, 28−37.
(32) Pan, J.; Xu, G.; Ding, B.; Han, J.; Dou, H.; Zhang, X. Enhanced electrochemical performance of sulfur cathodes with a water-soluble binder. *RSC Adv.* **2015**, *5*, 13709−13714.
(33) Kim, H. M.; Sun, H.-H.; Belharouak, I.; Manthiram, A.; Sun, Y.-K. An alternative approach to enhance the performance of high sulfur-loading electrodes for Li−S batteries. *ACS Energy Lett.* **2016**, *1*, 136−141.
(34) Chen, W.; Qian, T.; Xiong, J.; Xu, N.; Liu, X.; Liu, J.; Zhou, J.; Shen, X.; Yang, T.; Chen, Y.; et al. A new type of multifunctional polar binder: toward practical application of high energy lithium sulfur batteries. *Adv. Mater.* **2017**, *29*, 1605160.
(35) Chen, H.; Wang, C.; Dai, Y.; Qiu, S.; Yang, J.; Lu, W.; Chen, L. Rational design of cathode structure for high rate performance lithium-sulfur batteries. *Nano Lett.* **2015**, *15*, 5443−5448.
(36) Wu, F.; Lee, J. T.; Nitta, N.; Kim, H.; Borodin, O.; Yushin, G. Lithium iodide as a promising electrolyte additive for lithium-sulfur batteries: mechanisms of performance enhancement. *Adv. Mater.* **2015**, *27*, 101−108.
(37) Wang, H.; Zhang, C.; Chen, Z.; Liu, H. K.; Guo, Z. Large-scale synthesis of ordered mesoporous carbon fiber and its application as cathode material for lithium−sulfur batteries. *Carbon* **2015**, *81*, 782−787.
(38) Zhou, W.; Xiao, X.; Cai, M.; Yang, L. Polydopamine-coated, nitrogen-doped, hollow carbon-sulfur double-layered core-shell structure for improving lithium-sulfur batteries. *Nano Lett.* **2014**, *14*, 5250−5256.
(39) Yin, L. C.; Liang, J.; Zhou, G. M.; Li, F.; Saito, R.; Cheng, H. M. Understanding the interactions between lithium polysulfides and N-doped graphene using density functional theory calculations. *Nano Energy* **2016**, *25*, 203−210.
(40) Guo, J.; Yang, Z.; Yu, Y.; Abruna, H. D.; Archer, L. A. Lithium-sulfur battery cathode enabled by lithium-nitrile interaction. *J. Am. Chem. Soc.* **2013**, *135*, 763−767.
(41) Qiu, Y.; Li, W.; Zhao, W.; Li, G.; Hou, Y.; Liu, M.; Zhou, L.; Ye, F.; Li, H.; Wei, Z.; et al. High-rate, ultralong cycle-life lithium/sulfur batteries enabled by nitrogen-doped graphene. *Nano Lett.* **2014**, *14*, 4821−4827.
(42) Song, J.; Xu, T.; Gordin, M. L.; Zhu, P.; Lv, D.; Jiang, Y.-B.; Chen, Y.; Duan, Y.; Wang, D. Nitrogen-doped mesoporous carbon promoted chemical adsorption of sulfur and fabrication of high-areal-capacity sulfur cathode with exceptional cycling stability for lithium-sulfur batteries. *Adv. Funct. Mater.* **2014**, *24*, 1243−1250.
(43) Tang, C.; Zhang, Q.; Zhao, M. Q.; Huang, J. Q.; Cheng, X. B.; Tian, G. L.; Peng, H. J.; Wei, F. Nitrogen-doped aligned carbon nanotube/graphene sandwiches: facile catalytic growth on bifunctional natural catalysts and their applications as scaffolds for high-rate lithium-sulfur batteries. *Adv. Mater.* **2014**, *26*, 6100−6105.
(44) Zhou, W.; Wang, C.; Zhang, Q.; Abruña, H. D.; He, Y.; Wang, J.; Mao, S. X.; Xiao, X. Tailoring pore size of nitrogen-doped hollow carbon nanospheres for confining sulfur in lithium-sulfur batteries. *Adv. Energy Mater.* **2015**, *5*, 1401752.
(45) Song, J.; Gordin, M. L.; Xu, T.; Chen, S.; Yu, Z.; Sohn, H.; Lu, J.; Ren, Y.; Duan, Y.; Wang, D. Strong lithium polysulfide

DOI: 10.1021/acsenergylett.7b00779
ACS Energy Lett. 2017, 2, 2591−2597

chemisorption on electroactive sites of nitrogen-doped carbon composites for high-performance lithium-sulfur battery cathodes. *Angew. Chem., Int. Ed.* **2015**, *54*, 4325−4329.
(46) Wang, H.; Yang, Y.; Liang, Y.; Robinson, J. T.; Li, Y.; Jackson, A.; Cui, Y.; Dai, H. Graphene-wrapped sulfur particles as a rechargeable lithium-sulfur battery cathode material with high capacity and cycling stability. *Nano Lett.* **2011**, *11*, 2644−2647.
(47) Zeng, F.; Wang, W.; Wang, A.; Yuan, K.; Jin, Z.; Yang, Y. S. Multidimensional polycation beta-cyclodextrin polymer as an effective aqueous binder for high sulfur loading cathode in lithium-sulfur batteries. *ACS Appl. Mater. Interfaces* **2015**, *7*, 26257−26265.
(48) Park, K.; Cho, J. H.; Jang, J. H.; Yu, B. C.; De La Hoz, A. T.; Miller, K. M.; Ellison, C. J.; Goodenough, J. B. Trapping lithium polysulfides of a Li−S battery by forming lithium bonds in a polymer matrix. *Energy Environ. Sci.* **2015**, *8*, 2389−2395.
(49) Bhattacharya, P.; Nandasiri, M. I.; Lv, D.; Schwarz, A. M.; Darsell, J. T.; Henderson, W. A.; Tomalia, D. A.; Liu, J.; Zhang, J. G.; Xiao, J. Polyamidoamine dendrimer-based binders for high-loading lithium−sulfur battery cathodes. *Nano Energy* **2016**, *19*, 176−186.
(50) Fu, Y.; Manthiram, A. Enhanced cyclability of lithium−sulfur batteries by a polymer acid-doped polypyrrole mixed ionic−electronic conductor. *Chem. Mater.* **2012**, *24*, 3081−3087.
(51) Xu, G.; Yan, Q.b.; Kushima, A.; Zhang, X.; Pan, J.; Li, J. Conductive graphene oxide-polyacrylic acid (GOPAA) binder for lithium-sulfur battery. *Nano Energy* **2017**, *31*, 568−574.
(52) Wang, H.; Sencadas, V.; Gao, G.; Gao, H.; Du, A.; Liu, H.; Guo, Z. Strong affinity of polysulfide intermediates to multi-functional binder for practical application in lithium−sulfur batteries. *Nano Energy* **2016**, *26*, 722−728.
(53) Zhang, S. S. Binder based on polyelectrolyte for high capacity density lithium/sulfur battery. *J. Electrochem. Soc.* **2012**, *159*, A1226−A1229.
(54) Barchasz, C.; Molton, F.; Duboc, C.; Lepretre, J. C.; Patoux, S.; Alloin, F. Lithium/sulfur cell discharge mechanism: an original approach for intermediate species identification. *Anal. Chem.* **2012**, *84*, 3973−80.
(55) Clark, R. J.; Cobbold, D. G. Characterization of sulfur radical anions in solutions of alkali polysulfides in dimethylformamide and hexamethylphosphoramide and in the solid state in ultramarine blue, green, and red. *Inorg. Chem.* **1978**, *17*, 3169−3174.
(56) Fu, Y.; Zu, C.; Manthiram, A. In situ-formed Li_2S in lithiated graphite electrodes for lithium−sulfur batteries. *J. Am. Chem. Soc.* **2013**, *135*, 18044−18047.
(57) Su, Y. S.; Fu, Y.; Cochell, T.; Manthiram, A. A strategic approach to recharging lithium-sulphur batteries for long cycle life. *Nat. Commun.* **2013**, *4*, 2985.
(58) Tao, X.; Wang, J.; Ying, Z.; Cai, Q.; Zheng, G.; Gan, Y.; Huang, H.; Xia, Y.; Liang, C.; Zhang, W.; et al. Strong sulfur binding with conducting magnéli-phase Ti_nO_{2n-1} nanomaterials for improving lithium−sulfur batteries. *Nano Lett.* **2014**, *14*, 5288−5294.
(59) Yang, C. P.; Yin, Y. X.; Guo, Y. G.; Wan, L. J. Electrochemical (de) lithiation of 1D sulfur chains in Li−S batteries: a model system study. *J. Am. Chem. Soc.* **2015**, *137*, 2215−2218.
(60) Sharma, R. A. Equilibrium phases in the lithium-sulfur system. *J. Electrochem. Soc.* **1972**, *119*, 1439−1443.
(61) Cunningham, P.; Johnson, S.; Cairns, E. Phase equilibria in lithium-chalcogen systems II. lithium-sulfur. *J. Electrochem. Soc.* **1972**, *119*, 1448−1450.
(62) Levi, M. D.; Salitra, G.; Levy, N.; Aurbach, D.; Maier, J. Application of a quartz-crystal microbalance to measure ionic fluxes in microporous carbons for energy storage. *Nat. Mater.* **2009**, *8*, 872−875.
(63) Levi, M. D.; Levy, N.; Sigalov, S.; Salitra, G.; Aurbach, D.; Maier, J. Electrochemical quartz crystal microbalance (EQCM) studies of ions and solvents insertion into highly porous activated carbons. *J. Am. Chem. Soc.* **2010**, *132*, 13220−13222.
(64) Fu, C.; Guo, J. Challenges and current development of sulfur cathode in lithium−sulfur battery. *Curr. Opin. Chem. Eng.* **2016**, *13*, 53−62.

DOI: 10.1021/acsenergylett.7b00779
ACS Energy Lett. 2017, 2, 2591−2597

Supporting Information

Polycation Binders – An Effective Approach towards Lithium Polysulfides Sequestration in Li-S Batteries

Haiping Su[a,b], Chengyin Fu[b], Yifan Zhao[c], Donghui Long[a], Licheng Ling[a], Bryan M. Wong[b,c], Jun Lu[d]* and Juchen Guo[b,c]**

[a.] State Key Laboratory of Chemical Engineering, East China University of Science and Technology, Shanghai, 200237, P. R. China
[b.] Department of Chemical and Environmental Engineering, University of California, Riverside, CA 92521, USA
[c.] Materials Science and Engineering Program, University of California, Riverside, CA 92521, USA
[d.] Chemical Sciences and Engineering Division, Argonne National Laboratory, Argonne, IL 60439, USA

Experimental Section

Materials: All materials in this study except the aqueous GO dispersion were purchased from Sigma-Aldrich and used without further purification. The aqueous GO dispersion was purchased from Graphenea Inc. and used as received.

Synthesis of the S-GO@C composites: The porous carbon sheets GO@C were synthesized using a templating approach through polymerization of melamine-resorcinol-formaldehyde (MRF) resin onto few-layer GO sheets, followed by carbonization and activation. In a typical synthesis, 2.86 g resorcinol and 4.22 g formaldehyde (from 37 wt. % aqueous solution) were co-dissolved in 30 mL deionized water (solution A), 3.28 g melamine and 6.32 g formaldehyde were co-dissolved in 30 mL deionized water (solution B) at 80 °C. 50 mL of the aqueous GO dispersion (4 mg mL^{-1}) was subsequently added into the mixed solution of A and B under ultra-sonication for 10 min. The mixture was then stirred at 80 °C for 24 h. The obtained MRF-coated GO sheets were filtered and dried at 80 °C overnight. The carbonization was carried out at 1000 °C in flowing Ar/H_2 (95/5) for 3 h with a heating ramp of 3 °C min^{-1} to obtain the GO@C sheets. The obtained GO@C has a sheet-like structure as shown in the scanning electron microscopic (SEM) images in **Figure S2**. The CO_2 activation was performed by placing 0.1 g of GO@C composite in a tube furnace under flowing argon and being heated to 900 °C with a heating rate of 5 °C min^{-1}. After the targeted temperature was reached, the activating CO_2 gas was introduced for a certain period of time (2 to 6 hours) in a flow rate of approximately 0.04 SCFM. At the end of activation, CO_2 gas was shifted to argon and the activated GO@C was allowed to naturally cool down to room temperature. The S-GO@C composites were prepared via heating the thoroughly mixed sulfur and GO@C at 155 °C for 10 h in argon environment. The comparisons of structural properties of GO@C from different activation time and the electrochemical performance of the S-GO@C composites are shown in **Figures S3-S5** and **Table S2**.

PDAT Synthesis via Anion Exchange Reaction: Poly(diallyldimethyl ammonium triflate) (PDAT) was synthesized through an anion exchange reaction using poly(diallyldimethyl ammonium chloride) (PDADMAC) and silver triflate (CF_3SO_3Ag). In a typical reaction, 0.64 g CF_3SO_3Ag was dissolved in 32 mL deionized water, 2 g PDADMAC (20 wt.% solution in water) was then added into the solution under agitation for 6 h. The obtained suspension was then centrifuged to remove the precipitation (AgCl), and the PDAT solution was obtained.

Polysulfide Adsorption Experiments: 2 mM Li_2S_8 solution was prepared by reaction of a designated amount of sulfur to Li_2S in anhydrous DOL/DME (1:1, v/v) at room temperature (according to reaction $7/8S_8 + Li_2S \rightarrow Li_2S_8$). The mixture was stirred overnight in the glovebox for complete conversion. The GO@C carbon host is mixed with binder PVP and PDAT, respectively, in a mass ratio of 2/1 (GO@C/binder) followed by drying to form the adsorbents. 20 mg of the obtained adsorbents were added to 5 mL of the 2 mM Li_2S_8 solution for adsorption immediately followed by filtration and UV-Vis spectroscopy, which was performed with UV−visible spectrophotometer (Horiba Aqualog).

Mass Measurement of S-GO@C Cathodes by EQCM: Electrochemical Quartz Crystal Microbalance (EQCM) measurements of the mass change of the S-GO@C cathodes during lithiation were undertaken using a Gamry eQCM 10M^{TM} Quartz Crystal Microbalance and 10 MHz Au-coated Quartz Crystal with an electrode area of 0.205 cm^2. The mass change of the electrode can be calculated by using the Sauerbrey equation:

$$\Delta f = -2\Delta m f^2 / A\left(\mu\rho_q\right)^{1/2} = -C_f \Delta m$$

Where Δf is the measured resonant frequency (Hz), f is the intrinsic crystal frequency, Δm is the mass change, ρ_q *i*s the density of quartz, μ is the shear modulus and A is the electrode area. In this system, the mass sensitivity factor (C_f) is 226 Hz cm^2 μg^{-1}, which is obtained from standard copper deposition experiment.

Materials Characterization: The morphology and microstructure of the cathode materials were observed with scanning electron microscopy (SEM, FEI NNS450). Nitrogen adsorption-desorption was performed using an ASAP 2020 instrument at 77 K. The specific surface area and the pore size distribution were calculated using the Brunauer-Emmett-Teller (BET) and non-local density functional theory (NL-DFT) methods, respectively. Thermal gravimetric analysis (TGA) was conducted on a TG instrument (TA-Q500) under argon protection at a heating rate of 10 °C min^{-1} from room temperature to 600 °C. The XPS spectra of lithiated porous carbon with different binders were collected on AXIS Supra using monochromatic Al K radiation (280 W). To avoid environmental contamination, the cells were dissembled in an argon-filled glovebox, and the lithiated S-GO@C samples were then transferred into the XPS ultra-high vacuum chamber within an integrated glovebox.

Electrochemical Tests: The slurry in all electrode preparation was prepared by mixing 80 wt.% active material, 10 wt.% carbon black (super C65) and 10 wt.% binder dissolved in deionized water. The slurry was coated onto an aluminum foil with a doctor blade and dried at 50 °C in vacuum overnight to obtain the S-GO@C electrodes. The average sulfur loading on these electrodes was from 1.5 to 2.0 mg cm^{-2}. The high sulfur loading (approximately 4 mg cm^{-2}) electrodes were prepared on porous carbon paper (Spectracarb 2050A-0550) current collector (**Figure S6**). The selection of carbon paper as the current collector for high-loading cathodes was based on a comparison with the performance of the same electrodes on Al current collector

(**Figure S7**). A previous report by Peng and coworkers also demonstrated that Al current collector in high-loading sulfur cathodes was prone to corrosion, and porous carbon current collectors not only were more stable but also provided a superior electrical connection in thick sulfur electrodes.[1] The electrolyte was 1 M LiTFSI dissolved in a mixture of DOL and DME (1:1 by volume) with 1.5 wt.% of $LiNO_3$. A Celgard 2400 membrane was used as the separator. The electrolyte to sulfur (E/S) weight ratio was carefully controlled to range from 12/1 to 78/1. For the electrode with ~ 4 mg cm^{-2} sulfur loading, the volume of electrolyte (E/S = 12/1) used in cell assembling was approximately 40 μL cm^{-2}. The charge-discharge tests were performed on an Arbin battery test station, and the CV analysis was conducted on a Gamry Interface 1000.

(1) H.-J. Peng, W.-T. Xu, L. Zhu, D.-W. Wang, J.-Q. Huang, X.-B. Cheng, Z. Yuan, F. Wei, Q. Zhang, *Advanced Functional Materials* **2016**, 26, 6351.

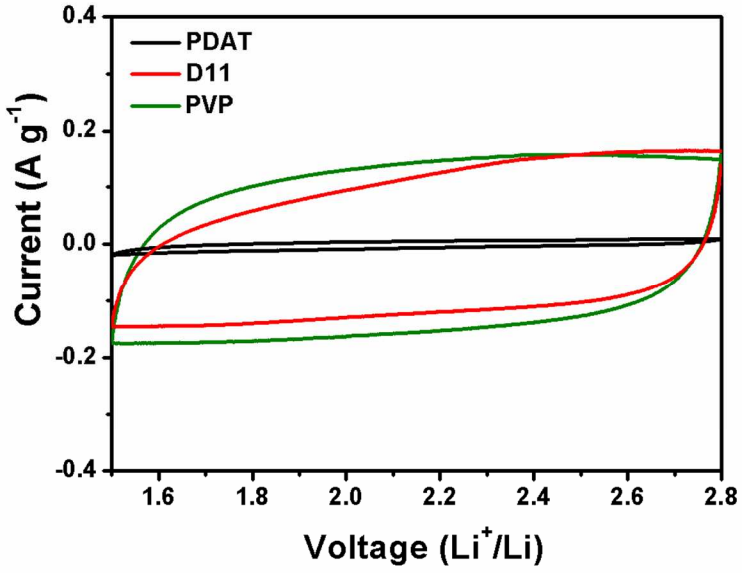

Figure S1. CV scans of the binder-GO@C composites between 1.5 and 2.8 V vs. Li^+/Li.

The tested electrodes were composed of the binders and the GO@C (S host) with a 1:2 weight ratio, which is the same as in the sulfur-carbon electrodes. The scan rate was 1 mV/s between 1.5 V and 2.8 V vs. Li reference electrode in 1 M LiTFSI in DOL/DME. It is clear that all three binders are stable within the typical electrochemical window of Li-S batteries indicated by the absence of redox characteristics in their CV scans. More interestingly, the three electrodes clearly show different capacitance due to the respective binders, 128.7 F/g for PVP-GO@C, 87.4 F/g for D11-GO@C, and 5.2 F/g for PDAT-GO@C, which is consistent with their capability as polysulfide anion adsorbents. The capacitance was based on the adsorption of Li^+ cations on the binder-GO@C composite, therefore, the lower capacitance indicates stronger cation repulsion from the binder, i.e., stronger adsorption of anionic polysulfide species. The CV results unambiguously demonstrate PDAT is the best binder for lithium polysulfide sequestration.

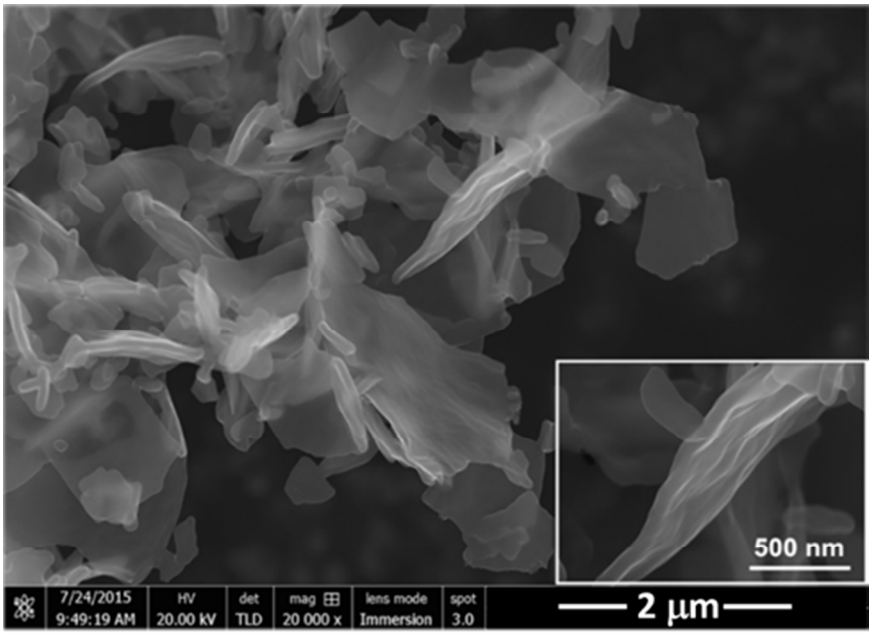

Figure S2. SEM images of non-activated GO@C.

To optimize the properties of the carbon host, the GO@C was activated with CO_2 at 900 °C for five different durations ranging from 2 to 6 hours (denoted as GO@C2H to GO@C6H). The specific surface area and pore volume of the porous GO@C (Figure S3 and Table S2) were increased with increasing duration of CO_2 activation from 500 m^2 g^{-1} (pristine GO@C) to 2775 m^2 g^{-1} (GO@C6H) and from 0.29 cm^3 g^{-1} (pristine GO@C) to 1.53 cm^3 g^{-1} (GO@C6H), respectively. Meanwhile, the pore size distribution (PSD) of the activated GO@C was also gradually broadened with the activation time as shown in Figure S3b. Sulfur was loaded in the activated GO@C hosts according to their theoretical content based on the specific pore volume. The actual sulfur loading agrees extremely well with the theoretical predictions as measured with thermogravimetric analysis (Figure S4). Among the five S-GO@C composites, S-GO@C2H had the lowest sulfur content of 60 wt.%, and S-GO@C6H had the highest sulfur content of 76.5 wt.%.

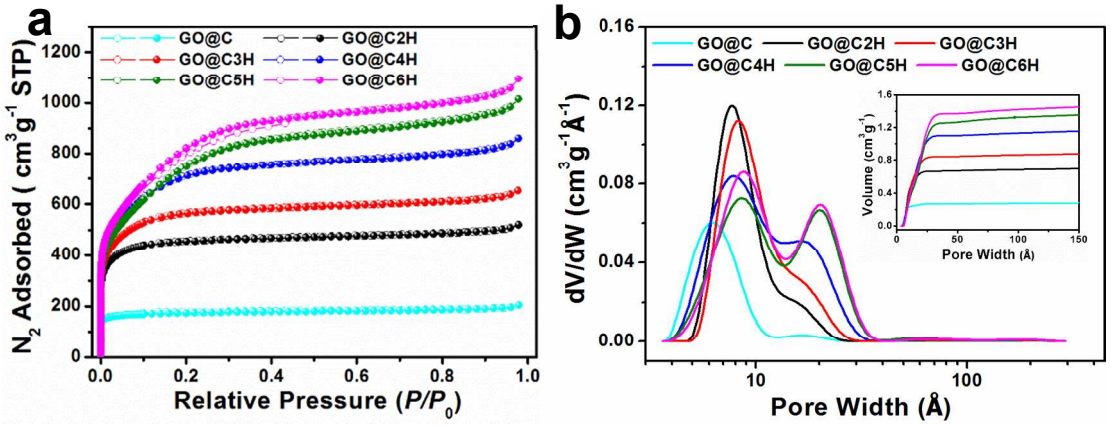

Figure S3. (a) N_2 adsorption-desorption isotherms of the pristine GO@C and the activated samples including GO@C2H, GO@C3H, GO@C4H, GO@C5H, and GO@C6H.; (b) PSD and specific pore volume of pristine GO@C and the activated GO@C.

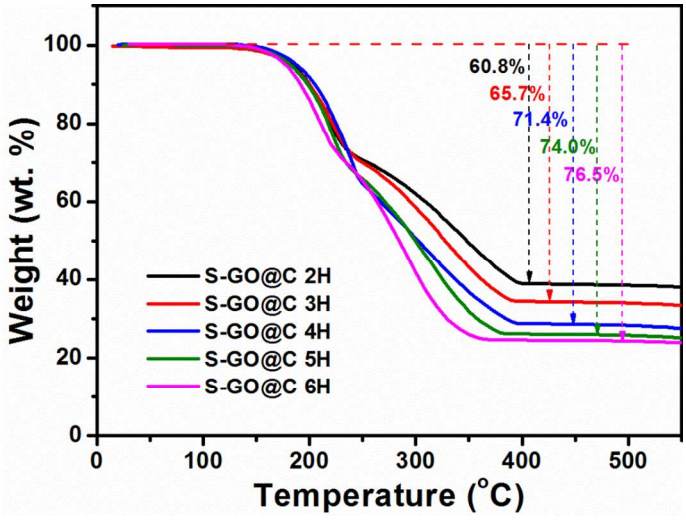

Figure S4. TGA curves of the sulfur loaded composites including S-GO@C2H, S-GO@C3H, S-GO@C4H, S-GO@C5H, and S-GO@C6H.

The electrochemical performance of the S-GO@C composites from different activation time were tested in electrodes composed of 80 wt.% composite, 10 wt.% carbon black and 10 wt.% PVP binder with E/S ratio of 50/1. The electrochemical data for each composite were obtained from the average of five individual cathodes tested under the same condition. The capacity vs. cycle number curves shown in Figure S5a demonstrate a clear correlation between the cathode performance and the structural properties of the GO@C hosts. The initial discharge capacity of the S-GO@C composites increases monotonically with increasing specific surface area and pore volume (i.e. sulfur loading): S-GO@C2H yields the lowest initial capacity at 500 mAh g^{-1}, while S-GO@C6H shows the highest one at 870 mAh g^{-1}. On the other hand, the stability is clearly determined by the PSD of the GO@C hosts: despite the highest initial capacity, S-GO@C6H, with the broadest PSD, displays the worst capacity retention. On the contrary, S-GO@C2H with the narrowest PSD shows the best capacity retention, although its overall capacity is too low to be practical. With the balanced specific surface area and PSD, S-GO@C5H (74 wt.% sulfur content) demonstrates the best overall performance. The CE data in Figure S5b also indicates a similar trend with S-GO@C5H demonstrating the best overall CE. *Therefore, S-GO@C5H was selected as the S-C composite in the reported studies in the manuscript, denoted as S-GO@C.*

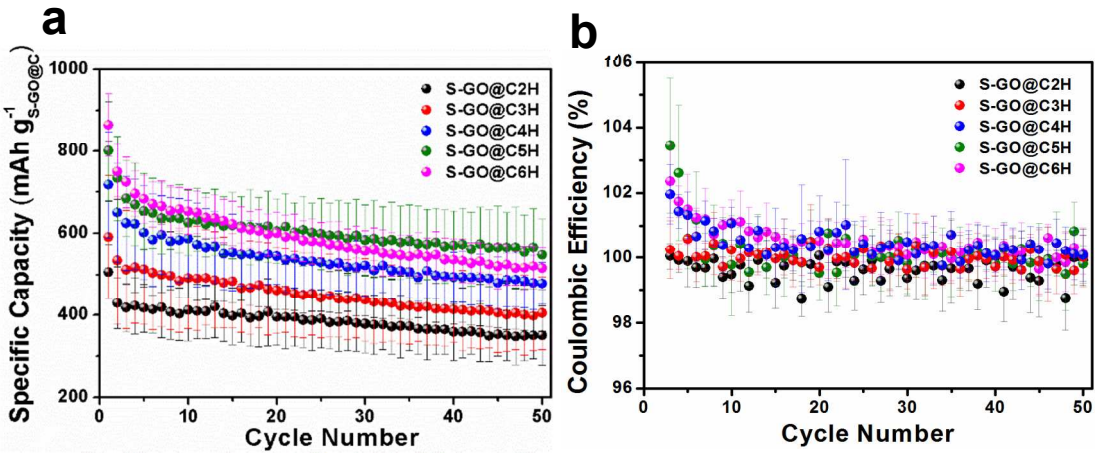

Figure S5. (a) capacity and cycling stability and (b) coulombic efficiency of the S-GO@C composites from S-GO@C2H to S-GO@C6H with PVP binder under 0.1 C rate and E/S ratio of 50/1.

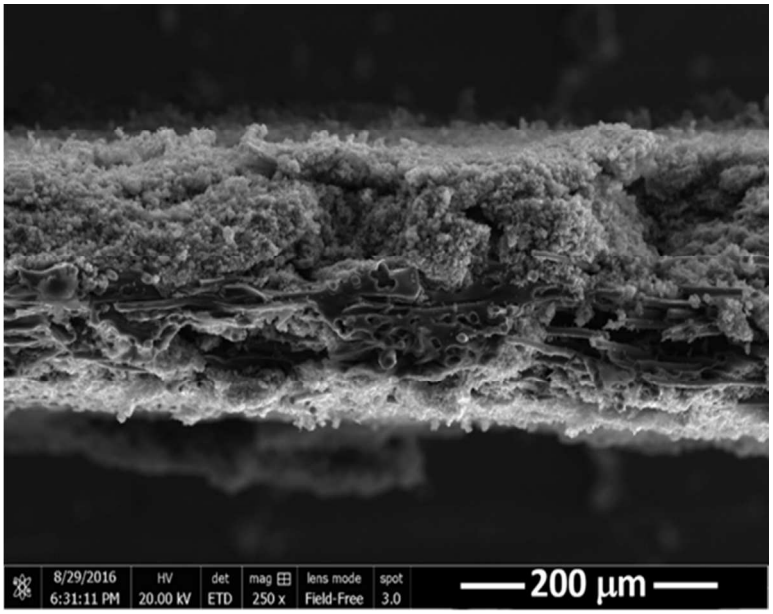

Figure S6. SEM of the high sulfur loading S-GO@C5H electrode with PDAT binder on carbon paper current collector.

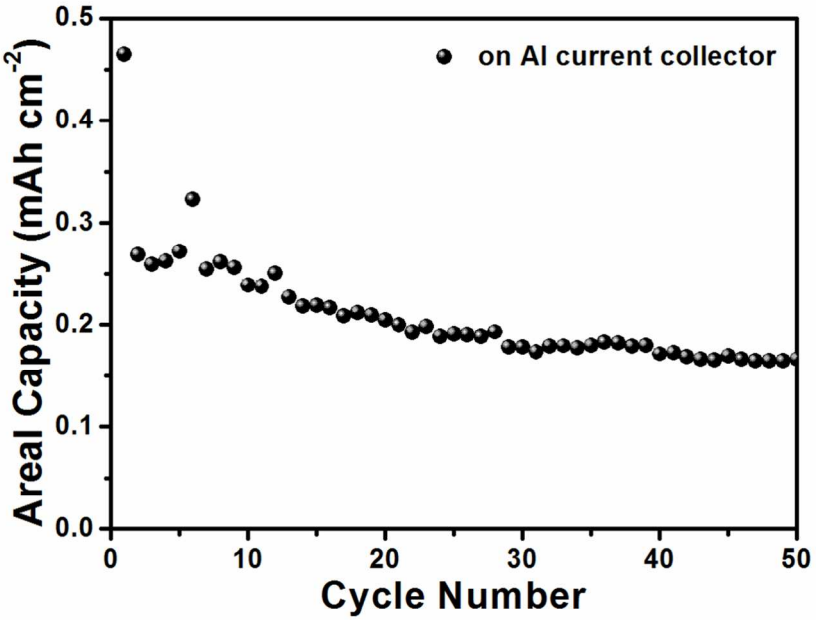

Figure S7. High sulfur loading (~ 4.2 mg cm^{-2}) S-GO@C5H electrode with PDAT binder on Al current collector with E/S ratio of 12/1.

Table S1. Elemental analysis of the sulfur content in polyquaternium D11. (The elemental analysis was performed by Elemental Analysis, Inc**)**

Sample ID	Sulfur (wt. %)
Polyquaternium D11	1.0%

The calculation of the cation concentration of the two polycation binders was based on their chemical formula. The formula weight of binder PDAT $(C_9H_{16}NSO_3F_3)_n$ and Polyquaternium D11 $(C_6H_9NO)_x(C_{12}H_{26}NSO_6)_y$ (x/y = 26) are 275 g mol^{-1} and 3198 g mol^{-1}, so the cation concentration are calculated to be $1/275 = 3.6\times10^{-3}$ mol g^{-1} and $1/3198 = 3.1\times10^{-4}$ mol g^{-1}, respectively.

Table S2. Specific surface area, specific pore volume, theoretical and actual sulfur loading of the GO@C hosts.

	S_{BET} (m^2 g^{-1})	V_t (cm^3 g^{-1})	**Sulfur Loading (theoretical)**	**Sulfur Loading (actual)**
GO@C	500	0.29	37.5%	N/A
GO@C2H	1313	0.73	60.2%	60.8%
GO@C3H	1651	0.91	65.3%	65.7%
GO@C4H	2187	1.20	71.3%	71.4%
GO@C5H	2496	1.42	74.7%	74.0%
GO@C6H	2775	1.53	76.0%	76.5%